

Supporting Information

Hollow spherical gold nanoparticle superstructures with tunable diameters and visible to near-infrared extinction

Chen Zhang,^{†*a*} Yong Zhou,^{†*b*} Andrea Merg,^{*a*} Chengyi Song,^{*a*} George C. Schatz,^{**b*} and Nathaniel L. Rosi,^{**a*}

^{*a*}Department of Chemistry, University of Pittsburgh, Pittsburgh, Pennsylvania 15260, United States. E-mail: nrosi@pitt.edu

^{*b*}Department of Chemistry, Northwestern University, Evanston, Illinois 60208-3113, United States. Email: schatz@chem.northwestern.edu

†Chen Zhang and Yong Zhou contributed equally to this work.

Supplementary Data

Materials and Methods: All solvents and chemicals were obtained from commercial sources and used without further purification. 0.1M HEPES Buffer (HEPES = 4-(2-hydroxyethyl)-1-piperazineethanesulfonic acid) was made by directly diluting 1.0 M HEPES buffer (pH = 7.3 ± 0.1; Fisher Scientific) with water (NANOpure, Barnstead Diamond™ System.; 18.2 MΩ). Peptide (AAAYSSGAPPMPPF or AA-PEP_{Au}) was synthesized and purified by New England Peptide with final purity of 99%. Reverse-phase high-pressure liquid chromatography (HPLC) was performed at ambient temperature with an Agilent 1200 liquid chromatographic system equipped with diode array and multiple wavelength detectors using a Grace Vydac protein C4 column (214TP1010, 1.0 cm × 25 cm). Matrix-assisted laser desorption ionization time-of-flight (MALDI-TOF) mass spectra were obtained using an Applied Biosystem Voyager System 6174 MALDI-TOF mass spectrometer using α -cyano-4-hydroxy cinnamic acid (CHCA) as the matrix. Transmission electron microscopy (TEM) samples were prepared by pipetting one drop of solution onto a 3-mm-diameter copper grid coated with carbon film; 2% aqueous phosphotungstic acid was used for negative staining. TEM was conducted on either a JEOL 200CX instrument operated at 200 kV and equipped with a Gatan CCD image system or FEI Morgagni 268 operated at 80kV and equipped with an AMT side mount CCD camera system. UV-Vis spectra were collected using an Agilent 8453 UV-Vis Spectrometer with a quartz cuvette (10 mm pass length) at room temperature.

Preparation of N-hydroxyl-succinimide esters and peptide conjugates

N-hydroxyl-succinimide esters: Caproic acid (1.16 g, 10.0 mmol) and N-hydroxysuccinimide (1.18 g, 10.3 mmol) were dissolved in 100 mL dry ethyl acetate under an argon atmosphere. After addition of dicyclohexyl carbodiimide (DCC) (2.16 g, 10.5 mmol) at 0 °C, the solution was stirred overnight at room temperature. The reaction mixture was processed by removing

the precipitate via filtration. The solvent was removed under reduced pressure and the crystalline residue was recrystallized from isopropanol (iPrOH) to yield the N-hydroxyl-succinimide ester (506 mg, 1.44 mmol, 25%).

Peptide conjugates: AAAYSSGAPPMPPF (1.20 mg, 8.80×10^{-7} mol) was dissolved in 60 μ L dimethylformamide (DMF). After addition of caproic N-hydroxyl-succinimide ester (0.6 mg, 2.81×10^{-6} mol) in 60 μ L DMF and 1 μ L Et₃N under stirring, the solution was stirred at room temperature for 17 h. Pure C₆-AA-PEP_{Au} was obtained by conducting reversed-phase HPLC eluting with a linear gradient of 0.05% formic acid in CH₃CN and 0.1% formic acid in water (5/95 to 95/5 over 30 min.) (Fig. S14). The molecular weight for C₆-AA-PEP_{Au} was confirmed by MALDI-TOF mass spectrometry (Fig. S15). The concentration of the peptide was determined spectrophotometrically in water/acetonitrile (1:1) using the molar extinction coefficient of tyrosine ($1280 \text{ M}^{-1}\text{cm}^{-1}$) at 280 nm.

Preparation of small spheres: Lyophilized C₆-AA-PEP_{Au} ($\sim 3.74 \times 10^{-8}$ mol) was completely dissolved in 125 μ L 0.05 M HEPES buffer (pH = 7.3 ± 0.1) in a plastic vial. This peptide solution was allowed to incubate at room temperature for 30 min. During the 30 min. incubation time, a fresh gold ion precursor solution was prepared: 0.1 M chloroauric acid (HAuCl₄) in 1.0 M triethylammonium acetate (TEAA; pH = 7.0) buffer was incubated for 10 min. at room temperature. Thereafter, this mixture was centrifuged (10 min., 5K rpm). After the 30 min. peptide solution incubation period, 0.6 μ L of the supernatant of the centrifuged gold ion precursor solution was added to the peptide conjugate solution. A small amount of black precipitate appears after ~ 2 s. At that point, the mixture was immediately vortexed for 1 min. and then left undisturbed at room temperature for one day. Products from multiple syntheses were studied using TEM and UV-Vis spectroscopy.

Preparation of medium spheres: Lyophilized C₆-AA-PEP_{Au} ($\sim 1.87 \times 10^{-8}$ mol) was completely dissolved in 125 μ L 0.1 M HEPES buffer (pH = 7.3 \pm 0.1) in a plastic vial. This peptide solution was allowed to incubate for 30 min. at room temperature. During the 30 min. incubation time, a fresh gold ion precursor solution was prepared: 0.1M chloroauric acid (HAuCl₄) in 1.0 M triethylammonium acetate (TEAA; pH = 7.0) buffer was incubated for 10 min. at room temperature. Thereafter, this mixture was centrifuged (10 min., 5K rpm). After the 30 min. peptide solution incubation period, 0.7 μ L of the supernatant of the centrifuged gold ion precursor solution was added to the peptide conjugate solution. A small amount of black precipitate appears after \sim 2 s. At that point, the mixture was immediately vortexed for 1 min. and then left undisturbed at room temperature for 3 days. Afterwards, 1 μ L of 0.1 M cetyltrimethylammonium bromide (CTAB) solution was added and then vortexed for 1 min., leading to the final concentration of 0.8 mM of CTAB. Products from multiple syntheses were studied using TEM and UV-Vis spectroscopy.

Preparation of large spheres: Lyophilized C₆-AA-PEP_{Au} ($\sim 1.87 \times 10^{-8}$ mol) was completely dissolved in 110 μ L 0.1 M HEPES buffer and 15 μ L 1.0 M TEAA buffer (pH= 7.3 \pm 0.1) in a plastic vial. This peptide solution was allowed to incubate for 30 min. Thereafter, 4 μ L of 0.01 M chloroauric acid (HAuCl₄) aqueous solution was added to the above solution. The mixture was immediately vortexed for 1 min. and then left undisturbed at room temperature for one day. Products from multiple syntheses were studied using TEM and UV-Vis spectroscopy.

Note on sphere syntheses: Some batch-to-batch variation in product was observed, in particular for the large spheres where we often observe a broad distribution of sphere diameters. We attribute this variation to the small reaction scale and the small amounts of added reagents.

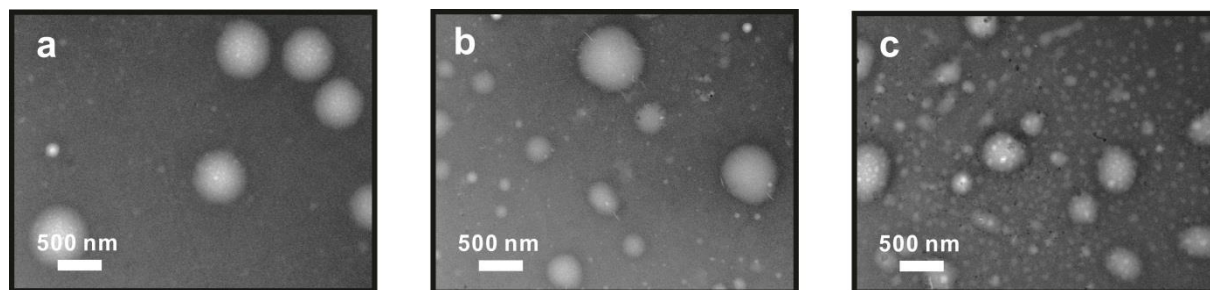


Figure S1. Negatively-stained TEM images of peptide conjugate assemblies at varied HEPES concentrations and incubation periods: a) 0.05 M of HEPES buffer, 1 day; b) 0.01 M of HEPES buffer, 6 h; 0.005 M of HEPES buffer, 30 min.

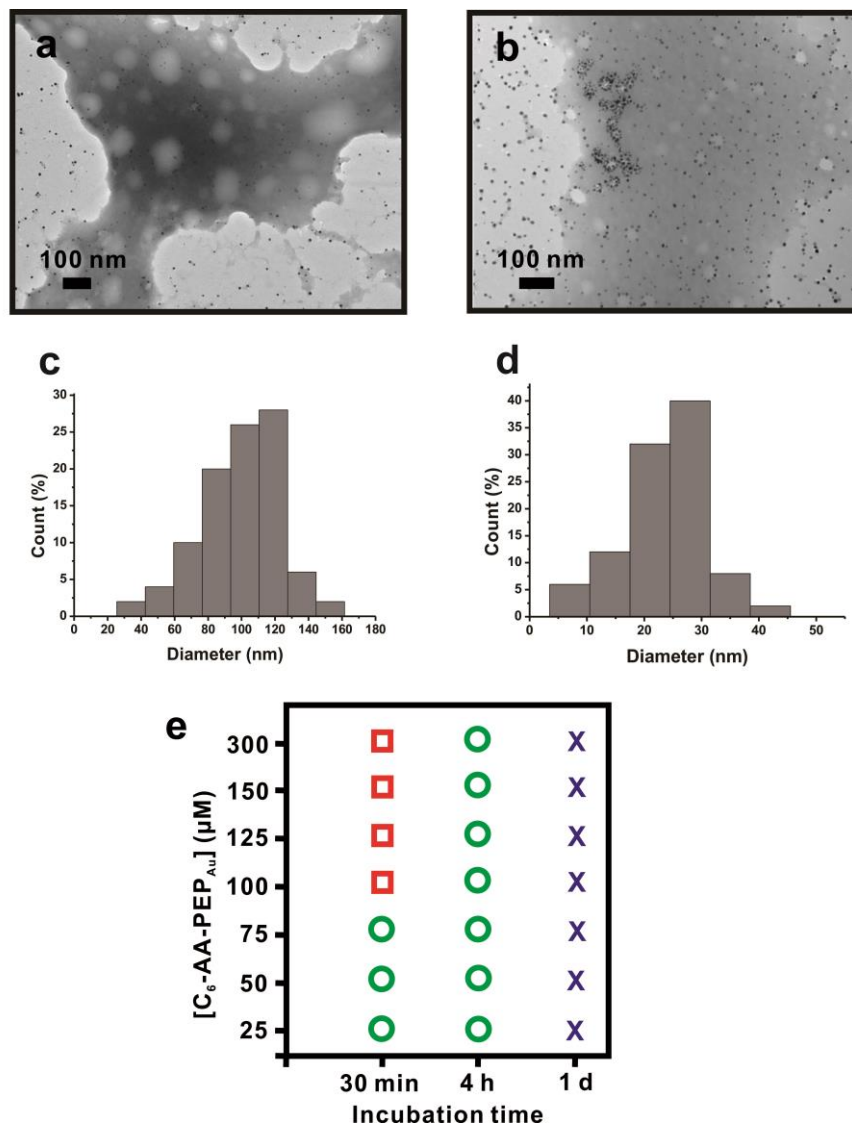


Figure S2. (a) Negatively-stained TEM images of peptide conjugate assemblies after adding HAuCl₄/TEAA and incubating at room temperature for 30 min. The concentration of C₆-AA-PEP_{Au} is 100 μM; (b) Negatively-stained TEM images of peptide conjugate assemblies after adding HAuCl₄/TEAA and incubating at room temperature for 30 min. The concentration of C₆-AA-PEP_{Au} is 25 μM; (c) Diameter distribution for image (a): 109 ± 21 nm, based on 100 counts; (d) Diameter distribution for image (b): 27 ± 8 nm, based on 100 counts; (e) Diagram summarizing peptide conjugate assembly in the presence of HAuCl₄/TEAA (incubation time versus concentration of C₆-AA-PEP_{Au}): red square, large spheres; green circle, small spheres; navy X, free nanoparticles and small spherical nanoparticle superstructures.

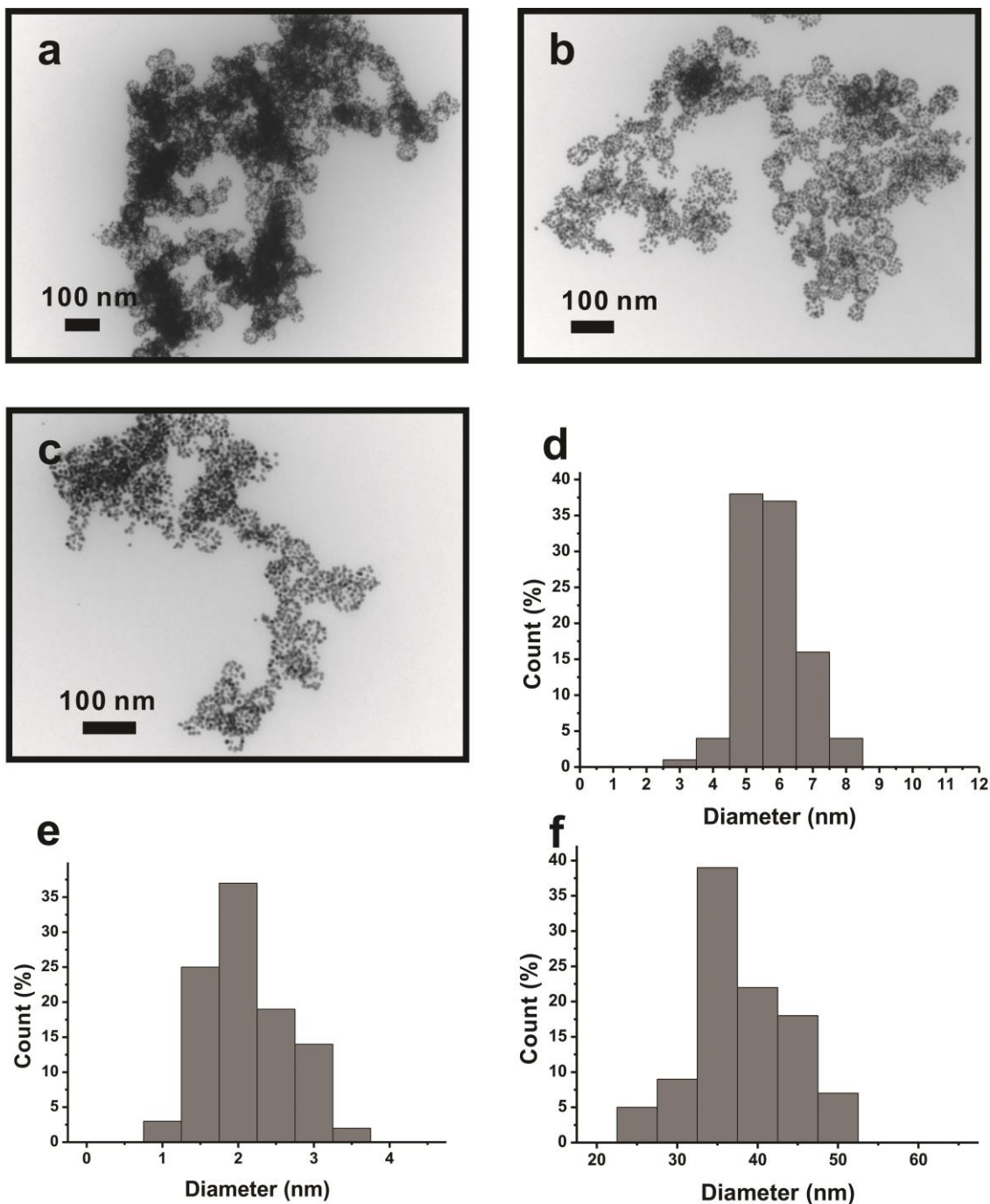


Figure S3. (a-c) TEM images of small spherical nanoparticle superstructures. (d) Distribution of gold nanoparticle diameter within the superstructures: 6.2 ± 0.9 nm, based on 100 counts; (e) Distribution of interparticle distances (gap) within the superstructures: 2.4 ± 0.6 nm, based on 100 counts; (f) Diameter distribution: 40.4 ± 5.9 nm, based on 100 counts. Note: these TEM images, along with those in Figure 1 of the manuscript, were obtained from multiple different sphere syntheses.

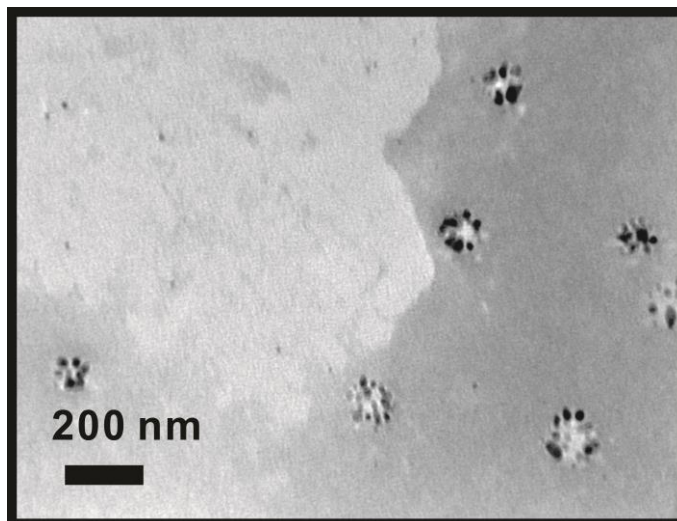


Figure S4. Negatively-stained TEM image of small spherical nanoparticle superstructures in 0.05 M of HEPES after adding $\text{HAuCl}_4/\text{TEAA}$ and incubating at room temperature for 4 hours.

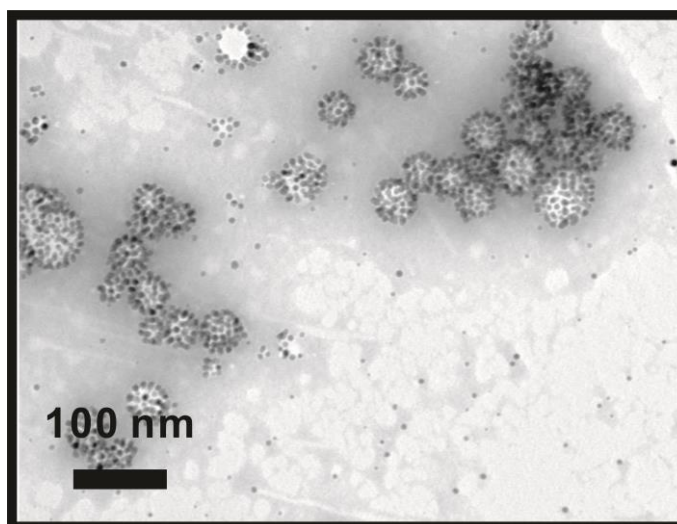


Figure S5. Negatively-stained TEM image of medium spherical nanoparticle superstructures after adding $\text{HAuCl}_4/\text{TEAA}$ and incubating at room temperature for 4 hours.

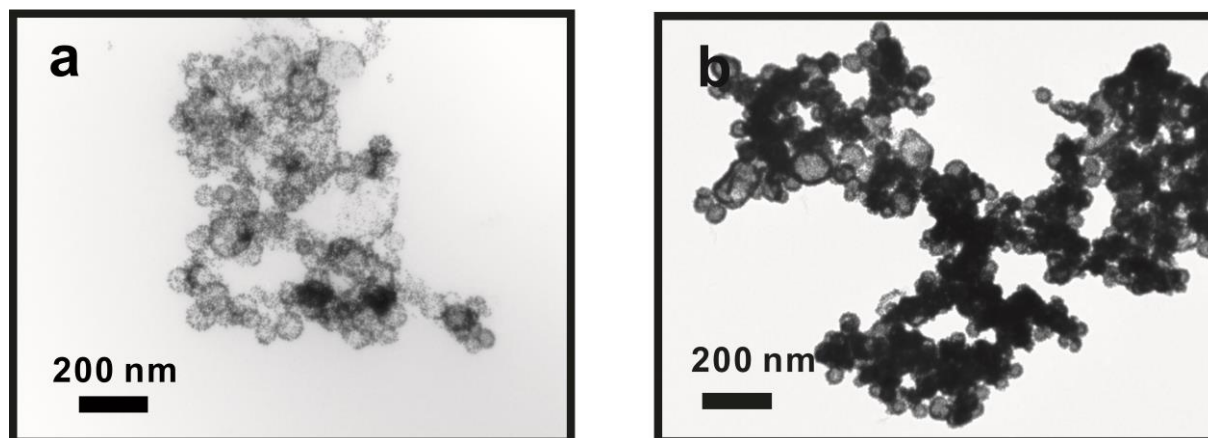


Figure S6. TEM image of medium spherical nanoparticle superstructures prepared using different amounts of $\text{HAuCl}_4/\text{TEAA}$ after one day of incubation at room temperature: a) 0.5 μL $\text{HAuCl}_4/\text{TEAA}$; b) 1.0 μL $\text{HAuCl}_4/\text{TEAA}$.

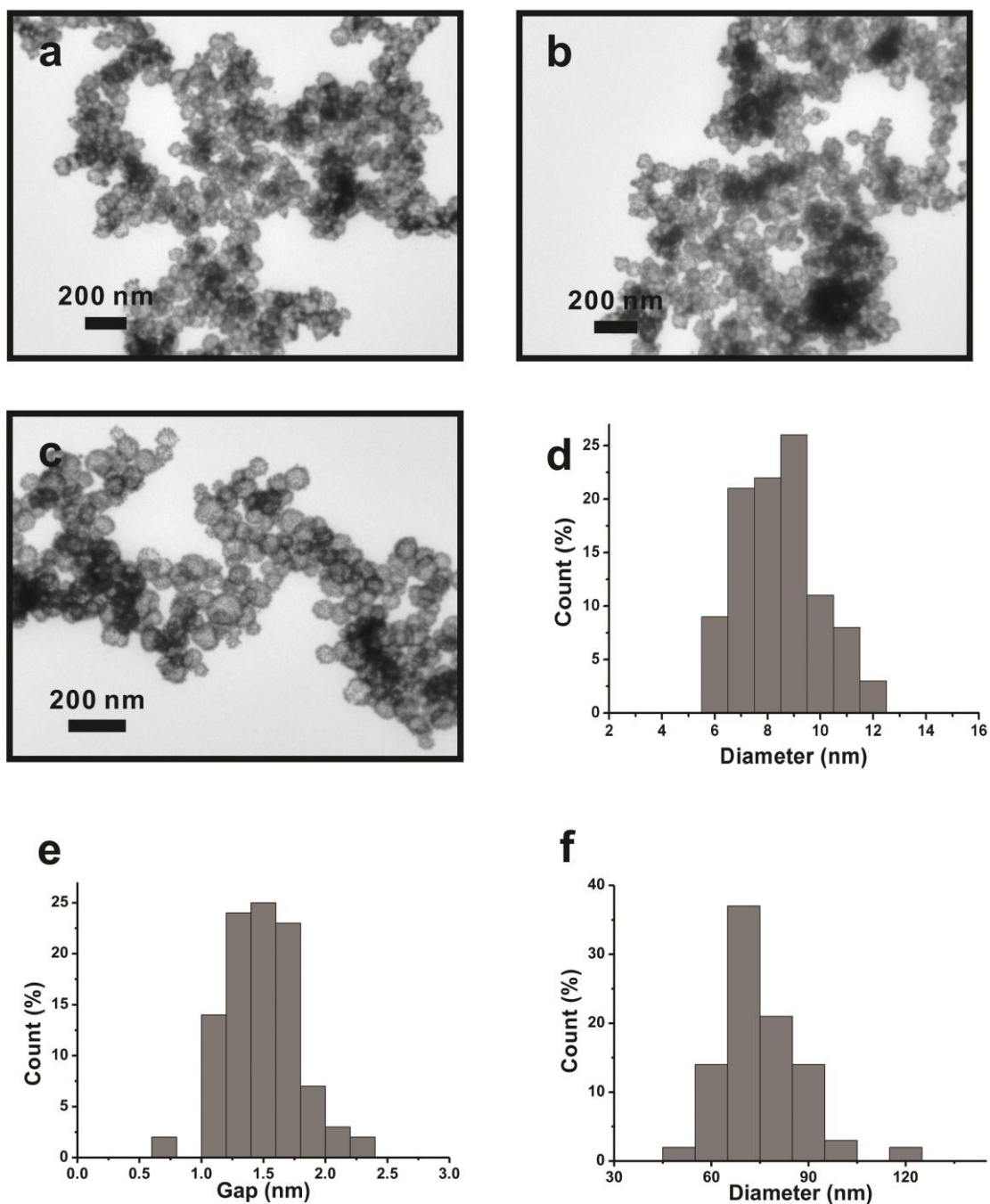


Figure S7. (a-c) TEM images of medium spherical nanoparticle superstructures. (d) Distribution of gold nanoparticle diameter within the superstructures: 8.5 ± 1.5 nm, based on 100 counts; (e) Distribution of interparticle distances (gap) within the superstructures: 1.5 ± 0.3 nm, based on 100 counts; (f) Diameter distribution: 75.3 ± 12.4 nm, based on 100 counts. Note: these TEM images, along with those in Figure 1 of the manuscript, were obtained from multiple different sphere syntheses.

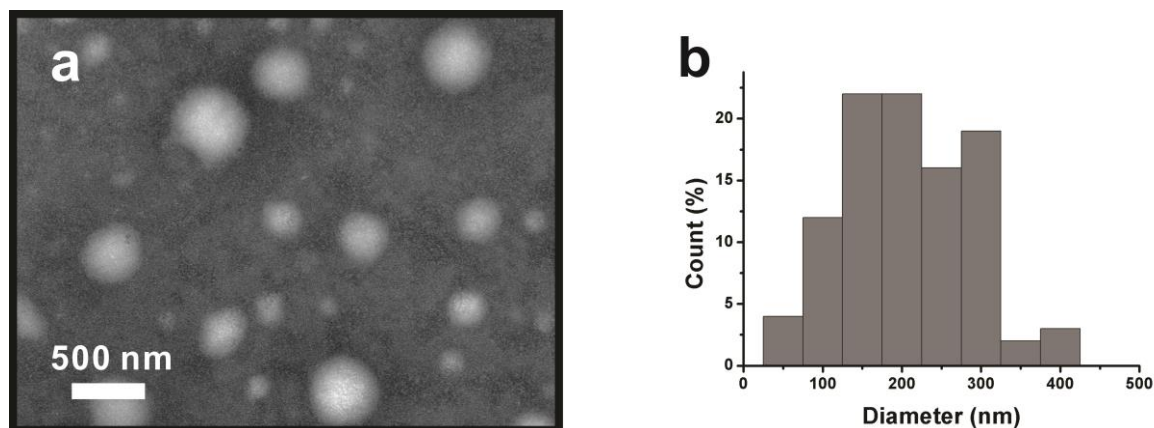


Figure S8. (a) Negatively-stained TEM images of C_6 -AA- PEP_{Au} assembly in HEPES/TEAA mixture after 4 hour incubation at room temperature; (b) Diameter distribution of these assemblies: 240 ± 81 nm, based on 100 counts.

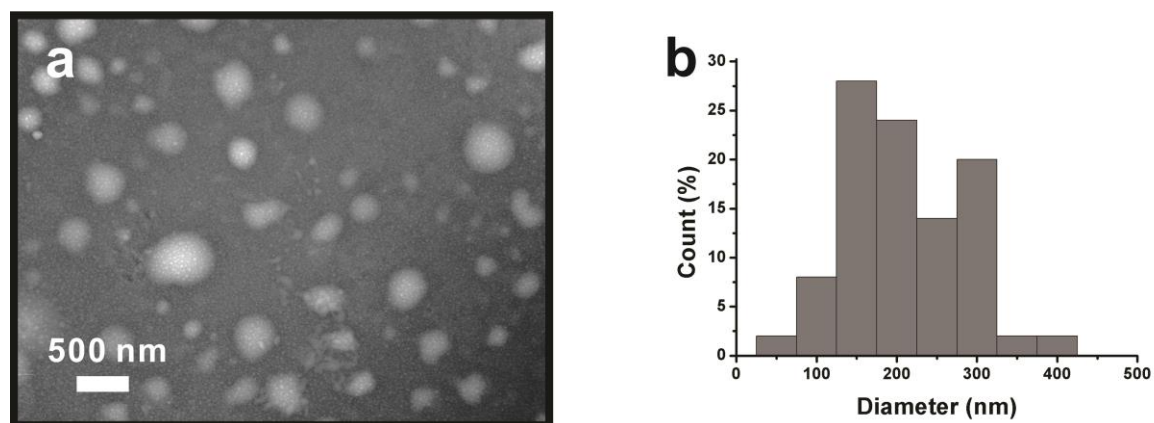


Figure S9. (a) Negatively-stained TEM image of C_6 -AA- PEP_{Au} assembly in HEPES/TEAA mixture after adding aqueous $HAuCl_4$ solution and incubating for 4 hours at room temperature; (b) Diameter distribution of these assemblies: 236 ± 75 nm, based on 100 counts.

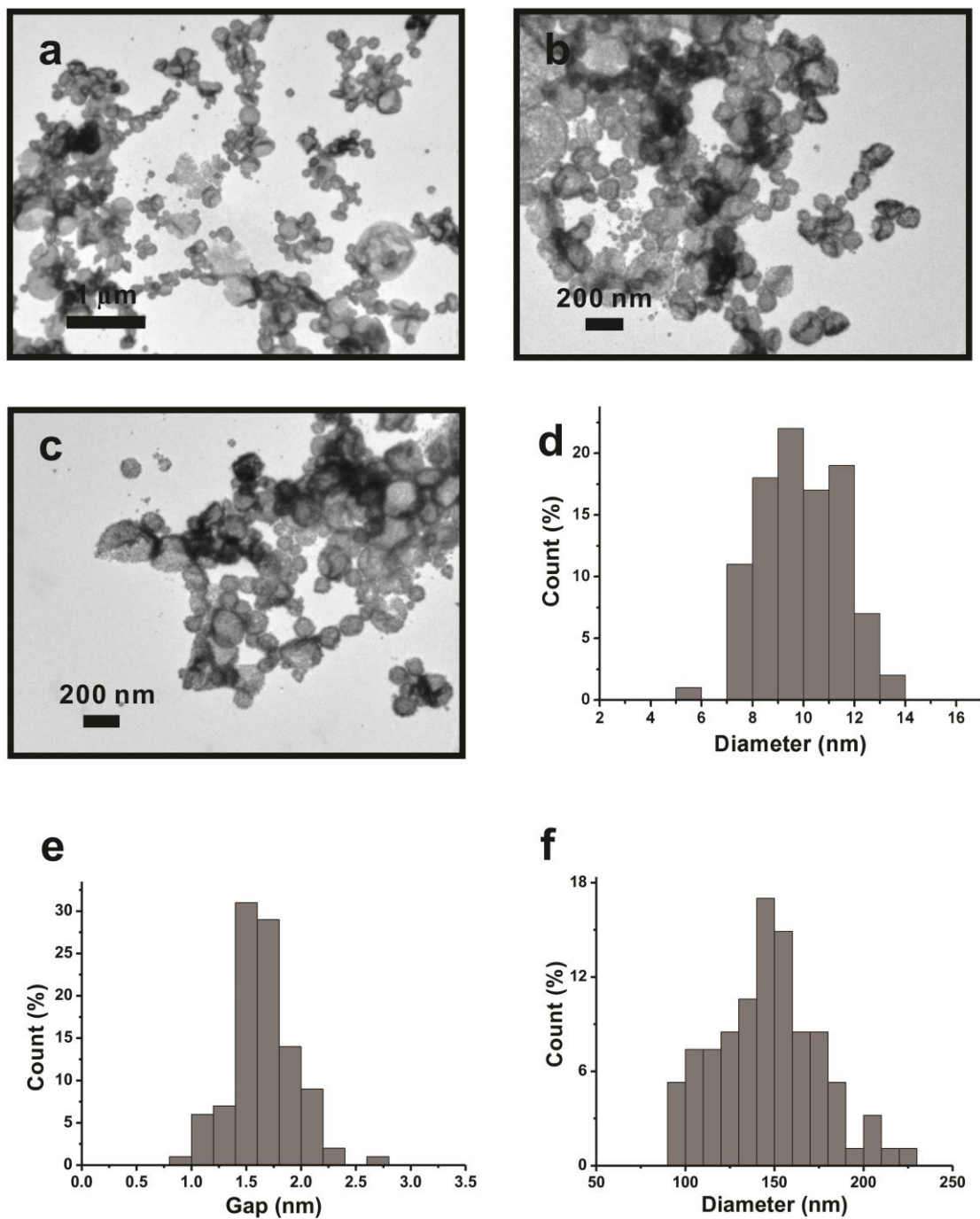


Figure S10. (a-c) TEM images of large spherical nanoparticle superstructures. (d) Distribution of gold nanoparticle diameter within the superstructures: 9.9 ± 1.6 nm, based on 100 counts; (e) Distribution of interparticle distances (gap) within the superstructures: 1.6 ± 0.3 nm, based on 100 counts; (f) Diameter distribution: 149.7 ± 30.8 nm, based on 100 counts. Note: these TEM images, along with those in Figure 1 of the manuscript, were obtained from multiple different sphere syntheses.

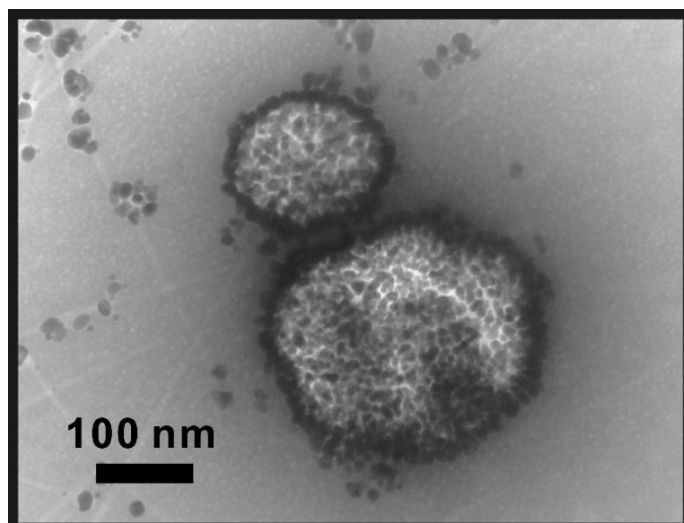


Figure S11. Negatively-stained TEM image of large spherical nanoparticle superstructures in HEPES/TEAA mixture after adding HAuCl_4 aqueous solution and incubating for 10 hours at room temperature.

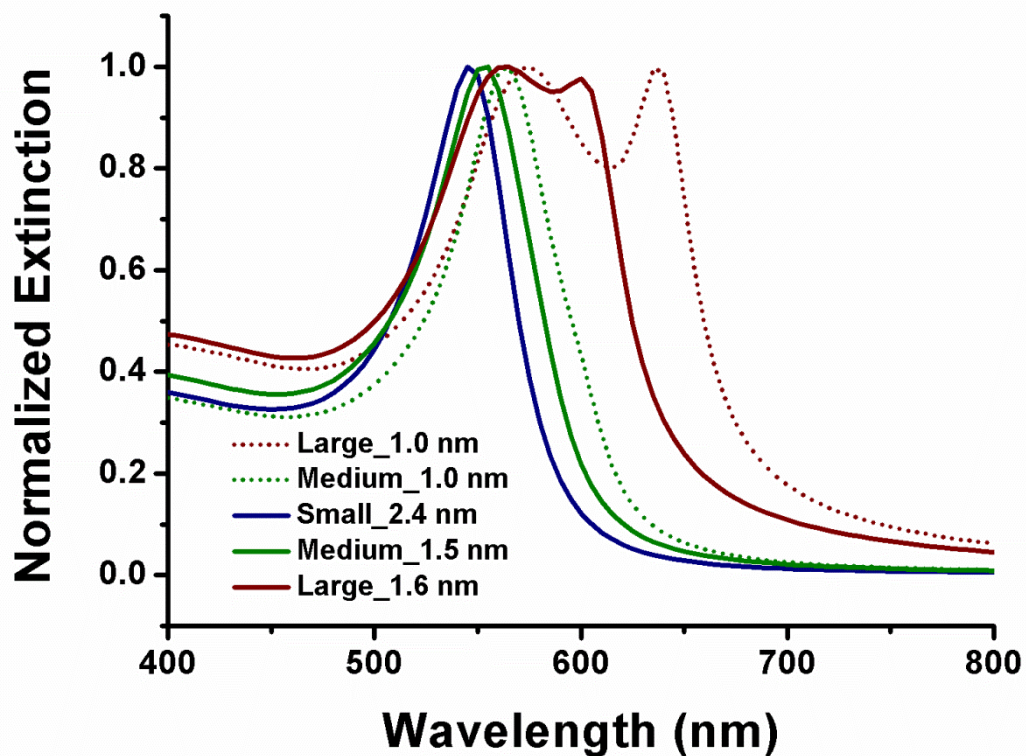


Figure S12. Extinction spectra of hollow spherical gold nanoparticle superstructures calculated using General Multiparticle Mie method. Component nanoparticles are assumed to be fully isolated in the simulation, with interparticle gaps from experimental measurement (see Table S1).

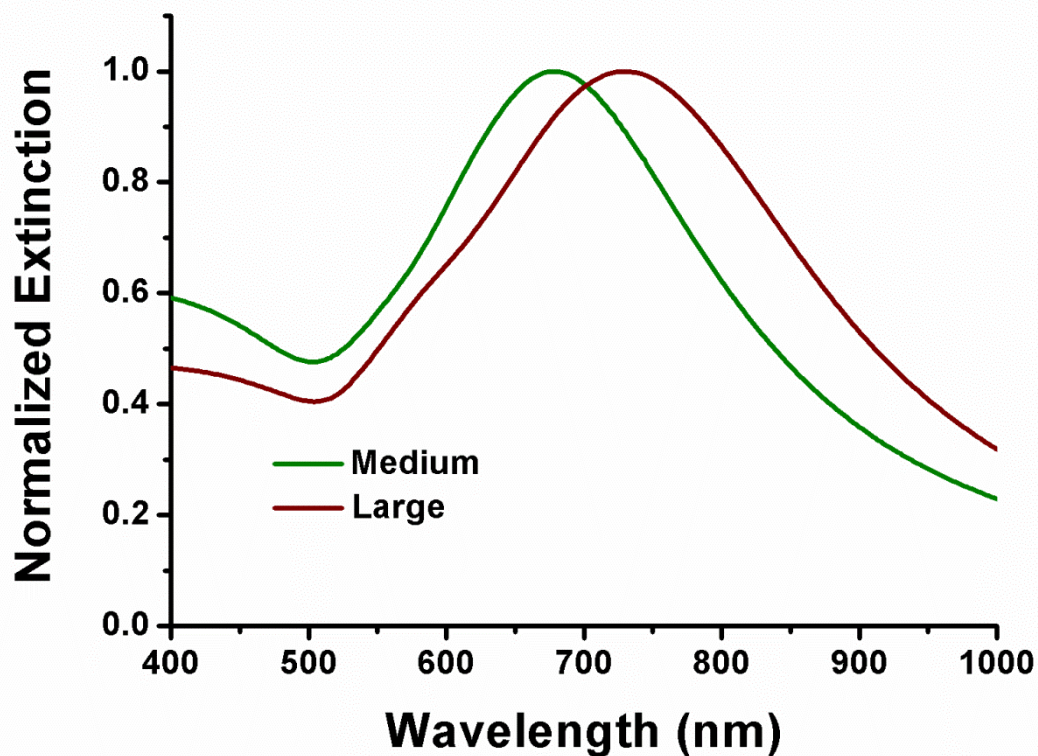


Figure S13. Extinction spectra of hollow spherical gold nanoparticle superstructures calculated using Mie theory. Component nanoparticles are assumed to be fused together. The spherical layer of gold nanoparticles is simplified as a continuous gold shell in the simulation, with the shell thickness determined by the average diameter of gold nanoparticles (see Table S1).

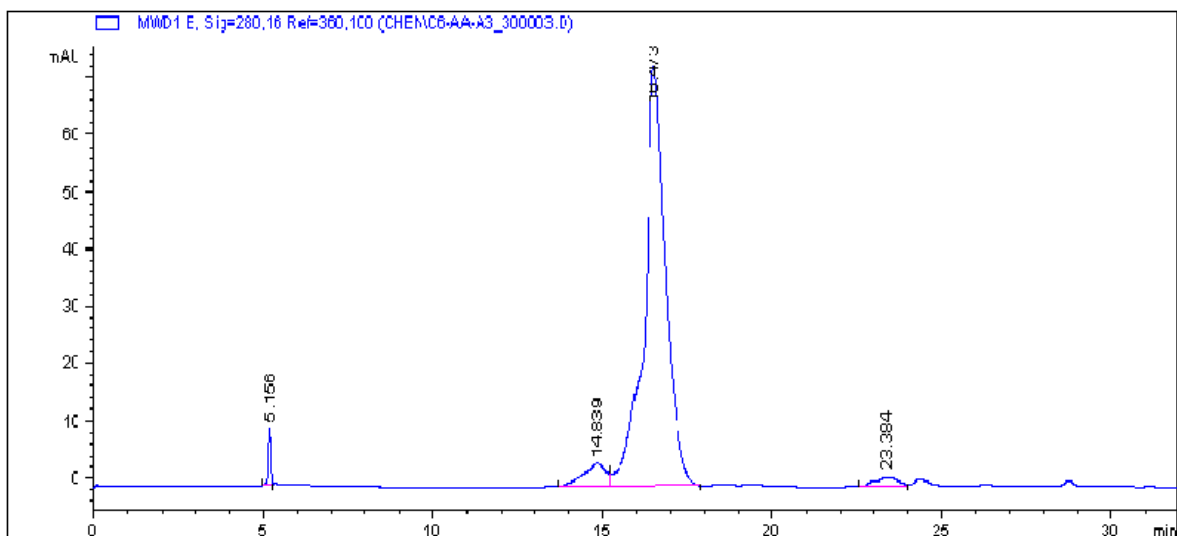


Figure S14. The reverse-phase HPLC chart for the coupling reaction of AAAYSSGAPMPPF with caproic N-hydroxyl-succinimide ester (retention time = 16.5 min).

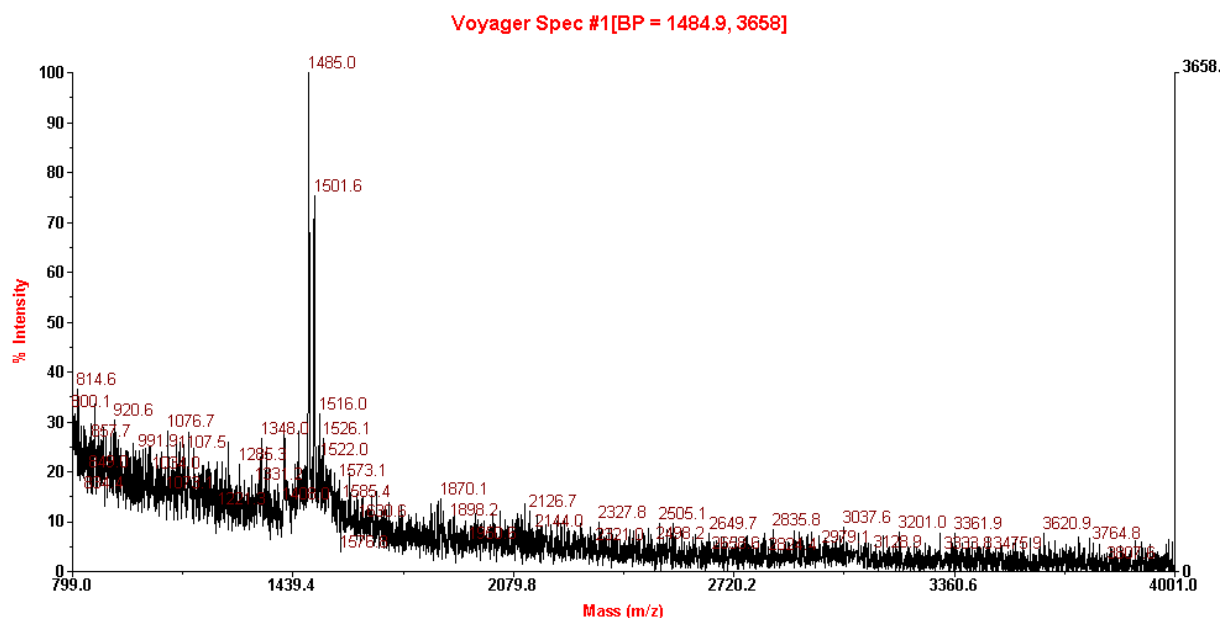


Figure S15. MALDI-TOF mass spectrum of purified C_6 -AA-PEP_{Au}. The molar mass of C_6 -AA-PEP_{Au} is 1462 g/mol. $[C_6$ -AA-PEP_{Au} + Na⁺] = 1485.0 g/mol and $[C_6$ -AA-PEP_{Au} + K⁺] = 1501.6 g/mol.

Table S1. Diameters of the superstructures, diameters of the gold nanoparticles (NPs), and observable interparticle distances (gaps).

Superstructures	Spheres [nm]	NPs [nm]	Gaps [nm]
Small	40.4 ± 5.9	6.2 ± 0.9	2.4 ± 0.6
Medium	75.3 ± 12.4	8.5 ± 1.5	1.5 ± 0.3
Large	149.7 ± 30.8	9.9 ± 1.6	1.6 ± 0.3